Effect of CNTs on morphology and electromagnetic properties of non-firing CNTs/silica composite ceramics

Bo PENG[Nagoya Institute of Technology], Chika TAKAI[Nagoya Institute of Technology],

Hadi RAZAVI-KHOSROSHAHI[Nagoya Institute of Technology], Montaser Sabbah El Din EL

SALMAWY[Suez University], Masayoshi FUJI[Nagoya Institute of Technology*],

*Corresponding author：Masayoshi FUJI

Advanced Ceramics Research Center, Nagoya Institute of Technology, Honmachi, 3-101-1, Tajimi,

Gifu, 507-0033, Japan

Tel.: +81 572 24 8110; fax: +81 572 24 8109.

E-mail addresses: fuji@nitech.ac.jp (M. Fuji).

Abstract： Carbon composite ceramics have much attention for industry because of their excellent properties such as strong toughness, high electrical conductivity as well as low percolation threshold. Therefore, carbon nanotubes (CNTs) were used to incorporate with silica ceramics in order to improve their electromagnetic properties. The amount of CNTs in CNTs/silica composite ceramics was varied in order to investigate its effect on morphologies and electromagnetic properties of those. The composites were successfully fabricated by non-firing process. The results revealed that the obtained CNTs/silica composite ceramic have an electrical resistivity of 66.6Ω•cm with a bending strength of 13.8Mpa. At the same time, the electromagnetic wave absorption ability achieved 70% over a wild frequency. This indicates that the CNTs in CNTs/silica composite ceramics may be potentially applied for an electromagnetic wave reflective material.

KEYWORDS: Non-firing ceramic; Carbon nanotubes; Mechano-chemical process; Electromagnetic property.

1. Introduction

Numerous research studies have investigated carbon nanotubes (CNTs) since Iijima announced the first observation of carbon nanotubes, which developed a new research field of one-dimensional carbon nano-materials [1]. CNTs show outstanding properties of excellent electricity [2,3], mechanics, such as high compressive strength [4,5], anisotropy of thermology [6-7], field emission characteristics [8], and also the adsorption ability of organic and inorganic pollutants [9-11]. These properties have attracted researchers' attention to synthesize carbon nanotubes composites such as the CNTs/metal matrix composite [12], CNTs/polymer matrix composite [13-17], and also CNTs reinforced ceramic composites [3,18-20]. Among the common synthetic materials, the CNTs/ceramic composites were supposed to enhance the electro-conductivity when compared with the original ceramic materials since it can confer a continuous electrical conductive path even with very low percolation thresholds. The research of CNTs by adding to ceramics as a conductive filler mainly focused on regulating the filler's concentration to improve conductivity, and also developing the appropriate fabrication method that can maintain a high aspect ratio

and the CNTs nanostructure which should always be regarded as one of the most important factors for the CNTs/ceramic composites.

As we have known, a high temperature sintering process is a necessary and common method for ceramic material preparation to insure a high relative density. However, both the sintering and calcination processes are not only consuming large amounts of non-renewable energy resources, but also possibly doing harm to the environment such as CO, SO_2 and dust emissions. Even if the spark plasma sinter (SPS) technology can effectively reduce the powder sintering temperature, it still has to be faced with a high power consumption and high pressure [20]. Moreover, especially for the CNTs/ceramic composite, the high sintering temperature may impact the carbon material nanotube microstructure and hamper the CNTs chemical or mechanical properties to some extent.

In order to solve these problems, research groups proposed an environmental friendly ceramic material fabrication method called a non-firing process [21,22]. The non-firing process means treating surface of raw ceramic powder by mechanical planetary ball mill activation [23] and continuously dispersing powder in an alkaline

solvent [24] to form precipitates and then eventually prepare ceramics solidified body. In addition, the fabrication processes should proceed at a much lower temperature (80^{o}C) than the sintering method, so that it effectively achieves the effect of reducing cost and energy without requiring any other special sintering equipment.

The carbon material was believed to be then ultimate reinforcement of ceramic composites by incorporating it with the SiO_2 ceramic matrix. In this study, we prepared CNTs/silica composite ceramics by a non-firing process and investigated the influence of different CNTs weight percentages on the composite properties such as microstructure, morphology, mechanical behavior，electro-conductivity, and also *electromagnetic wave reflectivity* especially at the Ku-band frequencies.

2. Experimental details

2.1 Materials and Preparation

A planetary ball mill with zirconia vials and zirconia balls (2 balls of Φ1.5cm and 25g of Φ0.5cm) was used to activate the amorphous SiO_2 (SO-C1, prepared by VMC method，Admatechs Company Limited) surface at a revolution rate of 200 r/m for 15 minutes. The single-walled carbon nanotubes in this study were well structured

with typical diameters in the range of 5-10 nm and an ideal length-diameter ratio of greater than 1,000 (Zeon Corporation). To prepare the ceramic composite, quartz powder (KS-100, F-plan) and raw CNTs were first mixed with a moderate amount of ethanol by a 30-minute sonication and 24-hour tumbler ball mill. For the next step, the solution was dried into powder via vacuum-rotary evaporation to remove the ethanol. The existence of quartz during the process made an attribute to not only prevent the shrinkage of the ceramic solid process, as well as dispersing the CNTs into solution.

The quartz/carbon nanotubes compounded powder was then mixed with activated SiO_2, and transferred into a resin tumbler bottle with small zirconia balls for 4 hours to ensure good mixing of the materials. After a sufficient tumbler ball milling, a 1 mol/L KOH solution was dropped to powder to prepare the ceramic slurry. Finally, slurry was mixed an electric mixer, and then kept 5 hours at 80^{o}C for it to solidify.

To investigate the effect of the CNTs amount on the ceramic composite, different carbon weight fraction of 0.07 %, 0.15 %, 0.30 % and 0.60 % in the blended silica powder were prepared. Amount of other components were listed in Table. 1.

2.2 Characterization

Raman spectrometer (NRS-3100, JASCO Corporation) was used to determine the graphitization and structural defects of carbon materials at room temperature. Scanning electron microscopy (SEM) (JSM-7000F, JEOL Limited) observed the morphology of the ceramic body and a transmission electron microscope (TEM) (JEM-2100F, JEOL Limited) investigated the combined structure between the SiO_2-SiO_2 particles and boundary between the CNTs-SiO_2 particles. For properties, the electrical conductivity was measured by the four-probe Van der Pauw method [25]. The three-point bending strength of the ceramic bulks was measured using a precision universal/tensile tester (AGS-G series, SHIMADZU Corporation.) with an average of 5 samples. The measurement proceeded at a 0.5% mm/min cross-head speed at room temperature, and the dimensions of the samples were fixed at 0.5 cm × 1cm × 5 cm (thickness × width × length). The electromagnetic wave reflectivity was measured by a free space method in the frequency range from 8.2-110.0 GHz (Microwave network analyzer, N5227A, Keysight Technologies).

3. Results and discussion

3.1 Raman spectra

The Raman spectra of the raw CNTs and silica-carbon nanotubes composite were measured to investigate the present condition of carbon in the composite (Fig. 1). The characteristic bands of the carbon material are the D-band and G-band, existing in the Raman shift at ~1350 cm^{-1} and 1550-1605 cm^{-1}, respectively. The G-band is an intrinsic feature associated with a high degree of symmetry and well ordered carbon nanotubes, which is closely related to the vibrations in all carbon materials formed by SP^2 hybridization. Meanwhile, the D-band is induced by disorder and defects [26].

As shown in Fig. 1, both the raw CNTs and composite show a higher intensity of the G-band compared to the D-band. The R-value (intensity ratio of D-band to G-band) determines the degree of graphitization. After calculating, The R-value of raw CNTs (R_{raw} = 0.37) is lower than that of silica-CNTs composite with 0.6 wt.% CNTs ($R_{1.0}$ = 0.97), which is mainly attributed to a symmetry-lowering effect due to defects, the presence of SiO_2 nanoparticles, and also the amorphous carbon produced during the ball milling process [27,28].

3.2 Morphology of composites

Typical SEM images of the CNTs-ceramic composite cross-section view are shown in Fig. 2. By increasing the amount of CNTs from (a) 0.07 wt.% to (b) 0.15 wt.%, (c) 0.30 wt. % and (d) 0.60 wt.%, it can be clearly observed that the carbon nanotubes effectively entangled into the silica matrix like bundles to form a network consisting of CNTs, which provide interlinked electro-conductive pathways among the composites. The samples presented three types of disorderly structures can be seen from high magnification images (e) and (f); i.e., inhomogeneous polyhedron quartz in (e), spherical silica nanoparticles combined with each other and a tube-like carbon material with about 10 nm diameter in (f). These three kinds of structures intersected with each other.

Focusing on Fig. 2 (d), the silica-CNTs composite possesses a superior and denser network microstructure than that of the lower CNTs amounts. The composite shows comparatively homogeneously dispersed carbon nanotubes in the silica matrix without affecting the formation and solidification of the ceramic base. Meanwhile, no more carbon material and a structure other than the nanotubes can be observed during the non-firing preparation process at a lower temperature than other sintering

processes.

Fig. 3 shows TEM images of the combined structure between the SiO_2-SiO_2 particles ((a) and (b)) and boundary between the CNTs- SiO_2 particles ((c) and (d)). With the addition of a certain amount of KOH (1 mol/L, 2.88g) into the silica-CNTs slurry, raw spherical and size inhomogeneous SiO_2 particles form a smooth internal combination between each other as shown in Fig. 3 (a) and (b), which ensures the physical properties of the ceramic material. After solidification, the residual KOH kept 0.71 wt.% in all samples. This morphology is highly consistent with the perspectives that planetary milling process leads to the occurrence of an activation reaction mechanism which means an increase in the specific surface activity of the amorphous silica powder [29], and also the slurry of the Si-rich pre-treated by the mechano-chemical activation should efficiently react with alkaline solution (in this work KOH) and form new chemical bonds [30]. Focusing on Fig. 3 (c) and (d), intimate contact between the nanotubes and silica combination structures was observed in this composite. During the formation of the SiO_2-SiO_2 continuum, carbon material still remained as bundles and tubes with a high draw ratio to determine the

CNTs network pathway structure.

3.3 Electro-conductivity and bending strength

The bending strength tested by the three-point method and electrical resistivity by the four-probe method are both shown in Figure. 4. The CNTs amount dependence of the electro-conductivity of the silica/CNTs amount can be apparently observed. The experimental results show that the electrical resistivity decreased with increasing CNTs amount, which suggests that the formation of the electro-conductive network made a contribution to ensuring electrons move freely in the material. After the CNTs were mixed into the silica, electro-resistivity rapidly decreased from 4574.2 Ω•cm to 1244.1 Ω•cm, and finally reached 66.6 Ω•cm, in the range of the semiconductor conductivity, which is close to the metallic conductor threshold after calculating to conductivity[31,32]. Non-firing process provided high-temperature and high-pressure [18] damaging carbon nanotubes stucture in composite by literature as high as 1300 ^{o}C to obtain electrical conductivity 10^{-10} s/cm with 0.23 vol.% (0.11 wt.%) , , and also decreasing the possibility of conversing to Si-C or Si-O-C, leading to incresing of electrical conductivity when compared to sintering process.

When the weight percentage of the CNTs increased, there is a slightly downward trend of the sample's bending strength. It can be considered that with the addition of carbon nanotubes, transferring of the stress inside ceramic matrix will loose on account of the weak interface between the CNTs and silica ceramic when compared with the non-CNTs ceramic materials. With a higher CNTs weight percentage in composite, agglomeration also increased, which affects the mechanical properties since it reduces the densification degree of the samples.

The bending strength is an important parameter for both the ceramic material and ceramic composite, in this case, focusing on improving the interface structure and decreasing the porosity should be an effective method to improve the mechanical properties.

3.4 Electromagnetic wave reflectivity

Since the free space method is a true and practical test for samples without requiring specific sizes and shapes, complete contact with a waveguide is also not required when compared to other methods [33]. As shown in Eq. (1), the power coefficient of the electromagnetic wave propagating in a material was described by

the Transmissivity (T), Reflectivity (R) and Absorptivity (A) [34]. In order to simplify the discussion, multi-reflection will not be considered here.

$$T + R + A = 1 \quad (1)$$

A schematic diagram of the experimental method is shown in Fig. 5. The electromagnetic wave as an incident wave enters the samples vertically and separates into three parts: reflection (R), absorption (A_1) and transmission (T_1). Since a metal obstacle is located on the backside of the sample, it can be assumed that the transmission part (T_1) reflects into the sample again without any energy loses and reflection. The absorption and transmission occur again in the sample being abbreviated as A_2 and T_2, respectively. The antenna setting in the vertical direction receives R and T_2 finally and was directly measured using a network analyzer. In conclusion, Eq. (2) is a redaction on based on of Eq. (1) shown below:

$$(A_1 + A_2) + (R + T_2) = 1 \quad (2)$$

In this study, the free space method was chosen to evaluate the electromagnetic wave shielding ability of the CNTs/silica composite ceramics with different CNTs amounts. This measurement covers a wide frequency range from 8.2 to 110.0 GHz,

and especially focusing on the frequency range from 12.0 to 18.0 GHz (Ku-band) shown in Fig. 6, which is used in the satellite communication field. Based on the results, the resonance of the absorption ratio occurs, which can be considered as the skin effect and the CNTs length to the incident wavelength. The absorption ratio also tends to be stable and as high as 90% has been achieved in the high frequency range. With the increase of CNTs weight percentage, absorption ratio of ceramic composite shows a decreasing trend. Combined with Eq. (1), it can be considered that the ability of $(R + T_2)$ gradually increasing with the increase amount of the CNTs. The composites show structural applications as a kind of effective material in the electromagnetic wave reflectivity filed .

4. Conclusions

By combining the mechano-chemical activation and reactive solution, an efficient and energy-saving process was proposed to fabricate functional ceramics without any calcination and sintering processes. By increasing the amount of incorporated CNTs, a continuous path was formed effectively to generate the electro-conductivity of ceramic material. The CNTs/silica composite ceramics show

an electromagnetic shielding ability with the increasing amount of the carbon material.

The silica-based ceramic materials fabricated in this study still have types of properties to be perfect, such as the mechanical strength and improvement of the electromagnetic wave reflective ability, while this research proposed and realized the probability of a functional ceramic material using a more facile and environmental method.

5. Acknowledgments

The authors gratefully acknowledge the CNTs support from the Zeon Corporation and A-STEP, JST (Adaptable and Seamless Technology transfer Program through target-driven R&D). We are also thankful for partial support by Knowledge Hub Aichi, Priority Research Project from the Aichi Prefectural Government.

6. Reference

[1] Iijima. S, Helical microtubules of graphitic carbon, Nature 354.6348 (1991) 56.

[2] T.W. Ebbesen, H.J. Lezec, H. Hiura, J.W. Bennett, H.F. Ghaemi, Electrical conductivity of individual carbon nanotubes, Nature 382 (1996) 54-56.

[3] S. Rul, F. Lefèvre-schlick, E. Capria, Ch. Laurent, A. Peigney, Percolation of single-walled carbon nanotubes in ceramic matrix nanocomposites, Acta Mater. 52 (4) (2004) 1061-1067.

[4] P.M. Ajayan, L.S. Schadler, C. Giannaris, A. Rubio, Single-walled carbon nanotube–polymer composites: strength and weakness, Adv. Mater. 12 (10) (2000) 750-753.

[5] A. Chaipanich, T. Nochaiya, W. Wongkeo, P. Torkittikul, Compressive strength and microstructure of carbon nanotubes–fly ash cement composites, Mater. Sci. Eng., A 527 (4) (2010) 1063-1067.

[6] A.M. Marconnet, N. Yamamoto, M.A. Panzer, B.L. Wardle, K.E. Goodson, Thermal conduction in aligned carbon nanotube–polymer nanocomposites with high packing density, ACS Nano, 5 (6) (2011) 4818-4825.

[7] R.S. Ruoff, D.C. Lorents, Mechanical and thermal properties of carbon nanotubes, Carbon 33 (7) (1995) 925-930.

[8] Q.H. Wang, T.D. Corrigan, J.Y. Dai, R.P.H. Chang, A.R. Krauss, Field emission from nanotube bundle emitters at low fields, Appl. Phys. Lett. 70 (24) (1997)

3308-3310.

[9] A.H. Norzilah, A. Fakhru'l-Razi, Thomas S.Y. Choong, A.L. Chuah, Surface modification effects on CNTs adsorption of methylene blue and phenol, J Nanomater 55 (2011).

[10] Y. Yao, F. Xu, M. Chen, Z. Xu, Z. Zhu, Adsorption behavior of methylene blue on carbon nanotubes. Bioresour. Technol. 101(9) (2010) 3040-3046.

[11] C.Y. Kuo, Water purification of removal aqueous copper (II) by as-grown and modified multi-walled carbon nanotubes, Desalin. 249(2) (2009) 781-785.

[12] C.D. Park, H.J. Jeon, H.J. Wang, Y.H. Choa, S.T. Oh, K.M. Kang, S.G. Kang, Synthesis of CNTs/Metal/Al_2O_3 nanocomposite powders by chemical vapor deposition. Mater. Sci. Forum 449 (2004) 797-800.

[13] H. Miyagawa, M. Misra, A.K. Mohanty, Mechanical properties of carbon nanotubes and their polymer nanocomposites, J. Nanosci. Nanotechnol, 5(10) (2005) 1593-1615.

[14] X. Zeng, S. Yu, L. Ye, et al. Encapsulating carbon nanotubes with SiO_2: a strategy for applying them in polymer nanocomposites with high mechanical

strength and electrical insulation[J]. Journal of Materials Chemistry C, 2015, 3(1): 187-195.

[15] L.Q. Zhang, B. Yang, J. Teng, et al. Tunable electromagnetic interference shielding effectiveness via multilayer assembly of regenerated cellulose as a supporting substrate and carbon nanotubes/polymer as a functional layer[J]. Journal of Materials Chemistry C, 2017, 5(12): 3130-3138.

[16] S. Zhao, J. Li, D. Cao, et al. Percolation threshold-inspired design of hierarchical multiscale hybrid architectures based on carbon nanotubes and silver nanoparticles for stretchable and printable electronics[J]. Journal of Materials Chemistry C, 2016, 4(27): 6666-6674.

[17] Y. Li, M. Li, M. Pang, et al. Effects of multi-walled carbon nanotube structures on the electrical and mechanical properties of silicone rubber filled with multi-walled carbon nanotubes[J]. Journal of Materials Chemistry C, 2015, 3(21): 5573-5579.

[18] J. Ning, J. Zhang, Y. Pan, J. Guo, Fabrication and mechanical properties of SiO_2 matrix composites reinforced by carbon nanotube, Mater. Sci. Eng., A, 357 (1)

(2003) 392-396.

[19] Y. Yang, M.C. Gupta, K.L. Dudley, Studies on electromagnetic interference shielding characteristics of metal nanoparticle-and carbon nanostructure-filled polymer composites in the Ku-band frequency. Micro. Nano Lett. 2 (4) (2007) 85-89.

[20] S.L. Shi, J. Liang, The effect of multi-wall carbon nanotubes on electro magnetic interference shielding of ceramic composites. Nanotechnology, 19 (25) (2008) 255707.

[21] T.T.T. Hien, T. Shirai, M. Fuji, An advanced fabrication route for alkali silicate glass by non-firing process. Adv. Powder Technol. 25(1) (2014) 360-364.

[22] E.U. Apiluck, T. Shirai, K. Tomoaki, K. Orito, H. Watanabe, M. Fuji, M. Takahashi, Novel fabrication route for porous ceramics using waste materials by non-firing process, J. Ceram. Soc. Jpn. 118 (1380) (2010) 745-748.

[23] G. Gorrasi, A. Sorrentino, Mechanical milling as a technology to produce structural and functional bio-nanocomposites, Green Chem. 17(5)(2015) 2610-2625.

[24] T. Shirai, K. Orito, T.T.T. Hien, M. Fuji, Effects of different forming methods on the properties of solidified body by non-firing process through the mechanochemical treatment, J. Jpn. Soc. Powder. Powder. Met. 59 (9) (2012) 517-521.

[25] M. Wakeshima, H. Masuda, K. Yamada, N. Sato, T. Fujino, New measurement system of specific resistivity and hall coefficient by four-probe van der pauw method, Tohoku University 52 (1/2) (1997) 135–144.

[26] M.S. Dresselhaus, G. Dresselhaus, A. Jorio, A.G. Souza Filho, R. Saito, Raman spectroscopy on isolated single wall carbon nanotubes, Carbon 40 (12) (2002) 2043-2061.

[27] K.E. Thomson, D. Jiang, R.O. Ritchie, A.K. Mukherjee, A preservation study of carbon nanotubes in alumina-based nanocomposites via Raman spectroscopy and nuclear magnetic resonance. Applied Physics A. 89 (3) (2007), 651-654.

[28] D. Jiang, K. Thomson, J.D. Kuntz, J.W. Ager, A.K. Mukherjee, Effect of sintering temperature on a single-wall carbon nanotube-toughened alumina-based nanocomposite. Scripta Mater. 56 (11) (2007) 959-962.

[29] T.T.T. Hien, T. Shirai, M. Fuji, Mechanical modification of silica powders, J. Cera. Soc. Jpn. 120 (1406) (2012) 429-435.

[30] W.K.W. Lee, J.S.J. van Deventer, Chemical interactions between siliceous aggregates and low-Ca alkali-activated cements, Cem. Concr. Res. 37 (6) (2007) 844-855.

[31] J.F. Shackelford, M.K. Muralidhara, Introduction to materials science for engineers (2005).

[32] G.D. Zhan, A.K. Mukherjee, Carbon nanotube reinforced alumina-based ceramics with novel mechanical, electrical, and thermal properties, Int. J. Appl. Ceram. Tec. 1 (2) (2004) 161-171.

[33] S. Geetha, K.K. Satheesh Kumar, C.R Rao, M. Vijayan, D.C. Trivedi, EMI shielding: methods and materials-a review, J. Appl. Polym. Sci. 112 (4) (2009) 2073-2086.

[34] S. Kwon, R. Ma, U. Kim, H.R. Choi, S. Baik, Flexible electromagnetic interference shields made of silver flakes, carbon nanotubes and nitrile butadiene rubber, Carbon 68 (2014) 118-124.

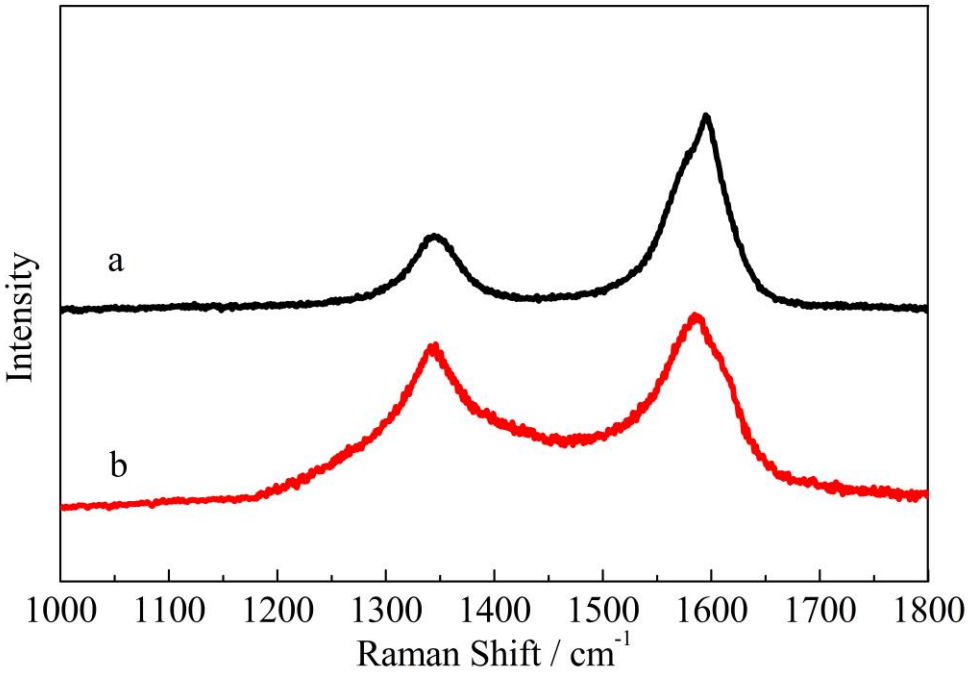

Fig. 1. Raman spectra of (a) raw carbon nanotubes and (b) silica-carbon nanotubes composite with 1.0 vol.% content of carbon nanotubes.

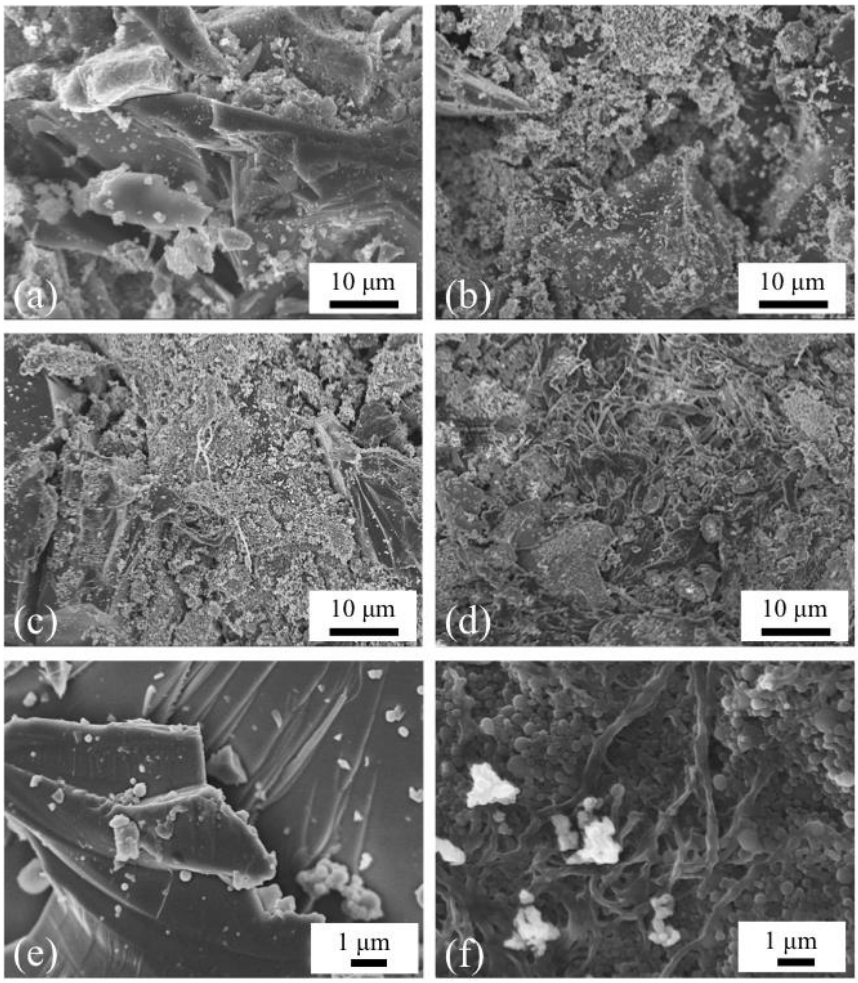

Fig. 2. SEM images of composite with different carbon nanotubes volume percentages from cross-section view. (a) 0.125 vol.% (b) 0.25 vol.% (c) 0.5 vol.% and (d) 1.0 vol.%. High magnification images of (e)(f) 1.0 vol.%

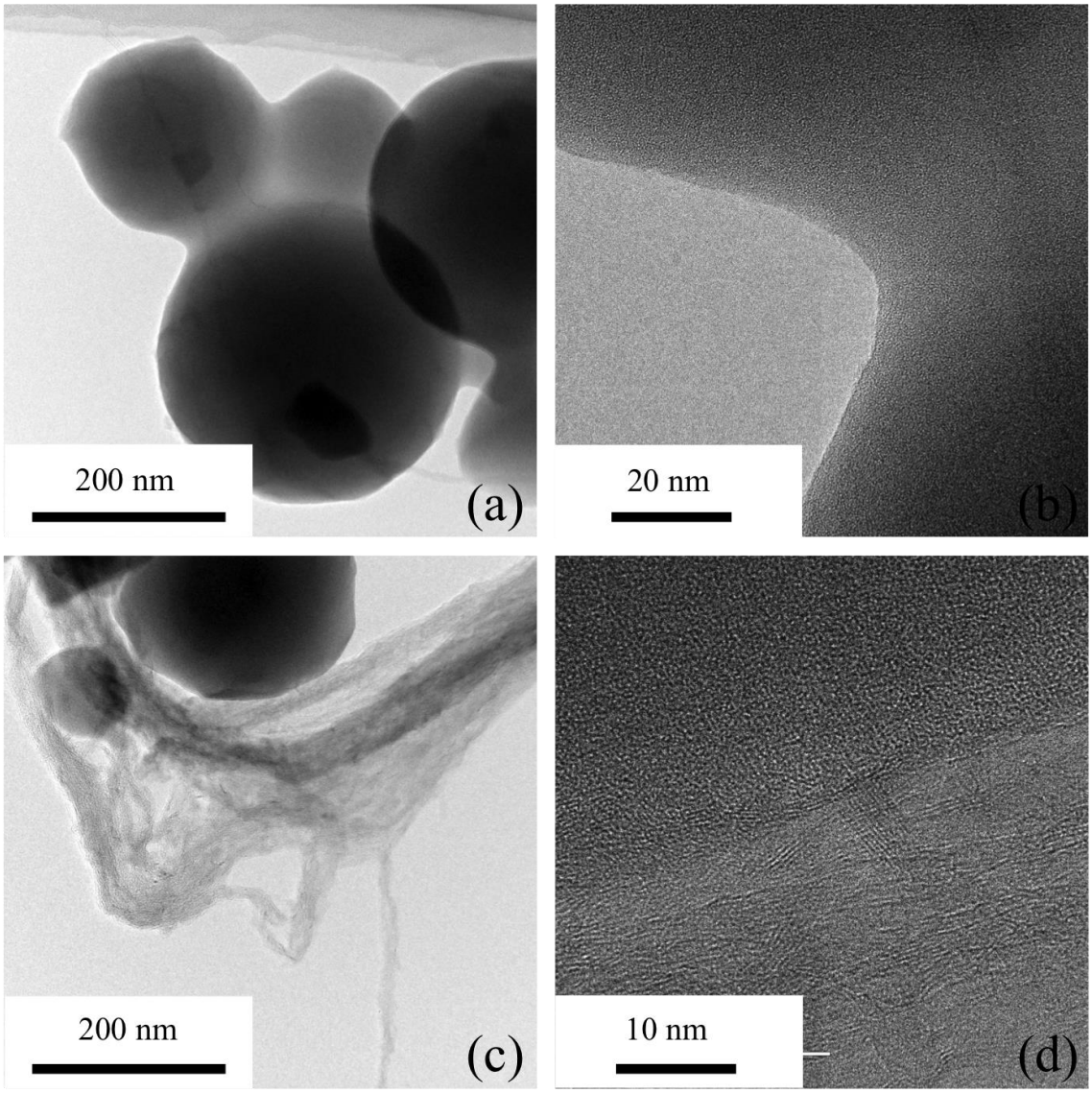

Fig. 3. TEM images of composite powders (a) combined structure between SiO_2-SiO_2 particles (low magnification) (b) combined structure between SiO_2-SiO_2 particles (high magnification) (c) boundary between CNTs- SiO_2 particles (low magnification) and (d) boundary between CNTs- SiO_2 particles (high magnification).

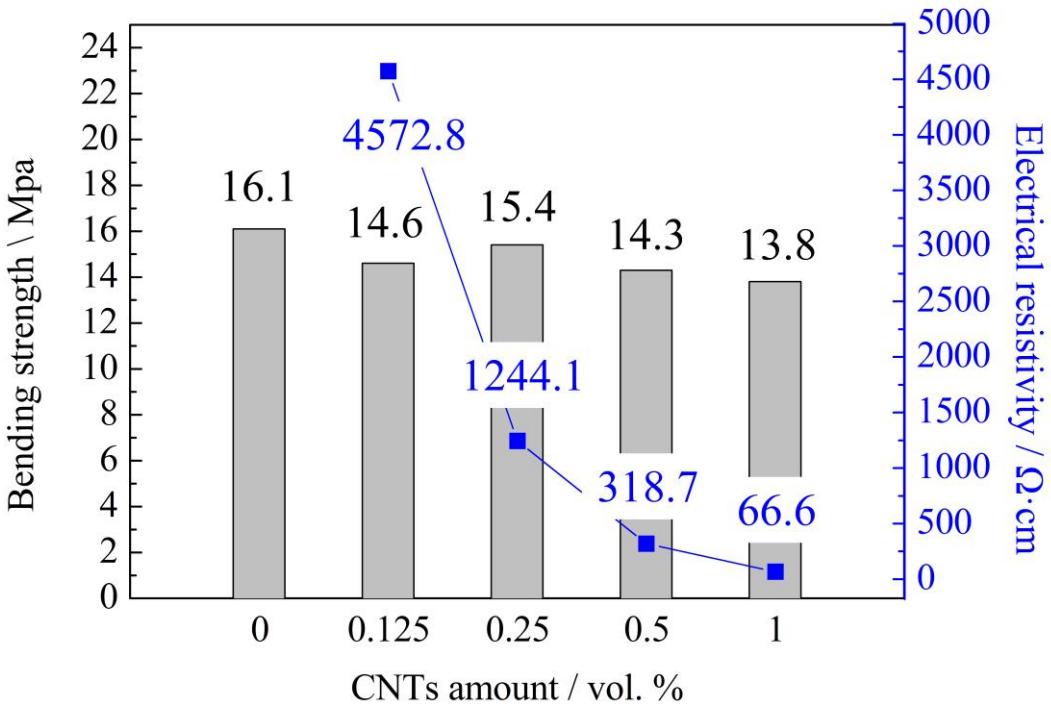

Fig. 4. Physical property of composites with different CNTs amounts (bending strength and electrical resistivity).

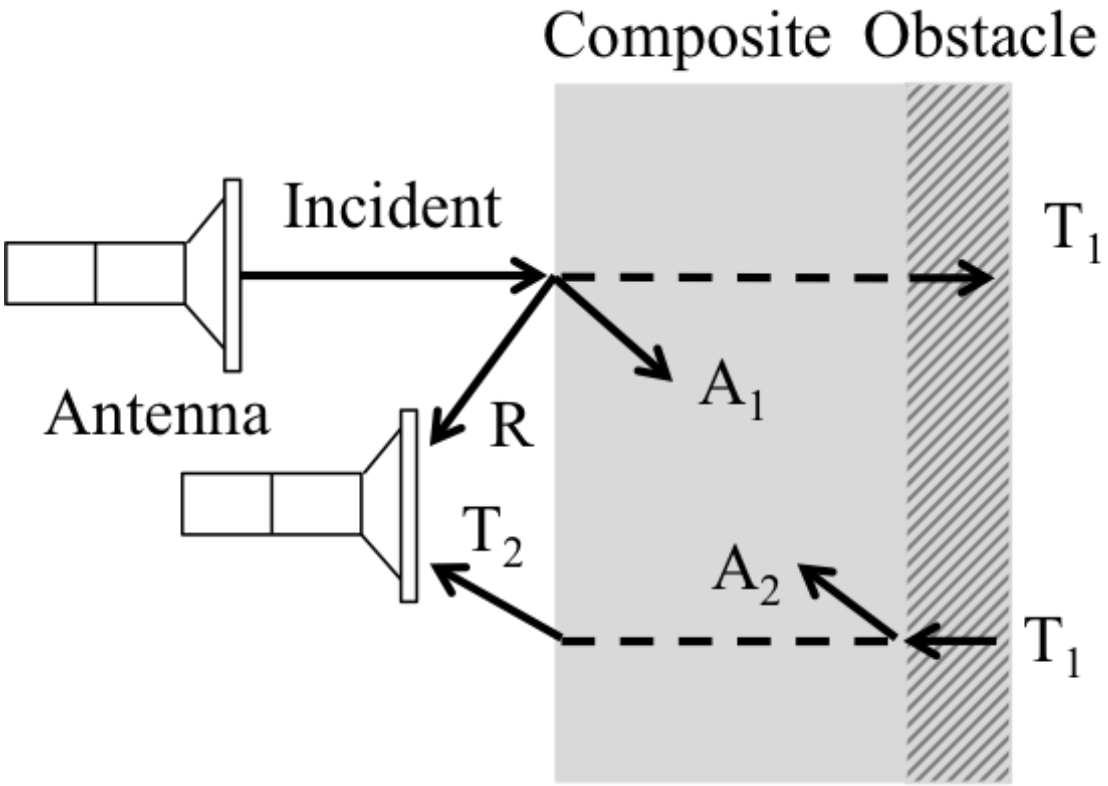

Fig. 5. Schematic of free space method.

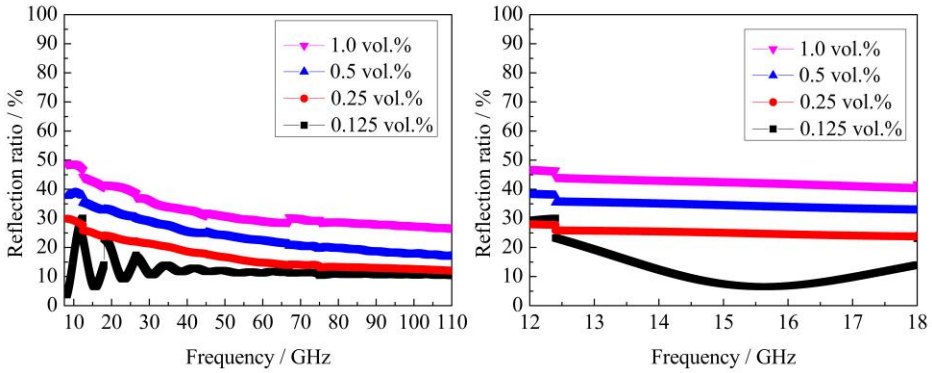

Fig. 6. Electromagnetic wave reflection ratio of CNTs/ceramic nanocomposites with different CNTs amounts.